



UNIVERSIDAD REGIONAL AMAZÓNICA IKIAM
FACULTAD DE CIENCIAS DE LA TIERRA Y AGUA
CARRERA EN HIDROLOGÍA

Proyecto de investigación previo a la obtención del título de Ingeniero en Ciencias
del Agua

**ANÁLISIS DE LA CONCENTRACIÓN Y DISTRIBUCIÓN DE PARÁMETROS FÍSICO
QUÍMICOS DEL EMBALSE SALVE FACCHA.**

Autor: Andrea Estefania Llumiquinga Suntaxi

Tutor: Jorge Emilio Celi Sangurima

Tena, febrero 2022.

Napo, Ecuador.

Declaración de derecho de autor, autenticidad y responsabilidad

Tena, 12 de octubre de 2021

Yo, Andrea Estefania Llumiquinga Suntaxi con documento de identidad N° 1717824104, declaro que los resultados obtenidos en la investigación que presento en este documento final, previo a la obtención del título Ingeniero en Ciencias del Agua, son absolutamente inéditos, originales, auténticos y personales.

En virtud de lo cual, el contenido, criterios, opiniones, resultados, análisis, interpretaciones, conclusiones, recomendaciones y todos los demás aspectos vertidos en la presente investigación son de mi autoría y de mi absoluta responsabilidad.

Por la favorable atención a la presente, suscribo de usted,

Atentamente,

Firma:



Andrea Estefania Llumiquinga Suntaxi
1717824104

Certificado de dirección de trabajo de integración curricular

Certifico que el trabajo de integración curricular titulado: “Análisis de la concentración y distribución de parámetros físico químicos del Embalse Salve Faccha”, en la modalidad de: Artículo original, fue realizado por: Andrea Estefania Llumiquinga Suntaxi, bajo mi dirección.

El mismo ha sido revisado en su totalidad y analizado por la herramienta de verificación de similitud de contenido; por lo tanto, cumple con los requisitos teóricos, científicos, técnicos, metodológicos y legales establecidos por la Universidad Regional Amazónica Ikiam, para su entrega y defensa.

Tena, 12 de octubre de 2021

Firma:



Firmado electrónicamente por:

**JORGE
EMILIO
CELI
SANGUR
IMA**

.....

Jorge Emilio Celi
Sangurima C.I:
1102662010
Tutor

AGRADECIMIENTOS

A mis padres, Lourdes y Luis por su apoyo en cada paso de mi vida, a mi hermana Eli, por todo lo compartido juntas, y a mis lindas criaturitas, por su calor en las épocas frías.

A mis amigos David, Ángel, Alex, Bryan y Diana, por convertirnos en una familia, y a Diego por ser siempre mi incondicional.

A los profes, por compartir su conocimiento y sembrar esa semilla de curiosidad, especialmente a mi tutor, por su apoyo en la realización de este trabajo.

Agradezco a la Estación Científica Agua y Páramo de la Empresa Pública Metropolitana de Agua Potable y Saneamiento (EPMAPS) Agua de Quito y Fondo para la Protección del Agua (FONAG) por la subvención y datos proporcionados para realizar el presente trabajo.

DEDICATORIA

A mi madre Lourdes, mi hermana Eli y mi abuelita Clementina, por ser las mujeres que me han inspirado para llegar hasta aquí.

ÍNDICE GENERAL

1. INTRODUCCIÓN	1
2. ÁREA DE ESTUDIO	1
3. MATERIALES Y MÉTODOS	3
3.1. Análisis meteorológico.....	3
3.2. Análisis de parámetros físico químicos.....	3
4. RESULTADOS	5
4.1. Meteorología	5
4.2. Patrones de alta frecuencia de parámetros físico-químicos	7
4.3. Patrones mensuales de parámetros físico-químicos.....	12
4.4. Correlación de Pearson.....	15
5. DISCUSIÓN.....	17
5.1. Patrones de alta frecuencia de parámetros físico-químicos	17
5.2. Patrones mensuales de parámetros físico-químicos.....	19
6. CONCLUSIÓN	20
7. AGRADECIMIENTOS	20
8. REFERENCIAS.....	21

ÍNDICE DE TABLAS

Tabla 1. Características de datos y periodo de estudio usados en el análisis meteorológico y de parámetros físico químicos.	4
Tabla 2. Resumen de estadísticas descriptivas de los datos recogidos por la hidroboya multiparamétrica de 2019 a 2020 a tres profundidades.	7
Tabla 3. Correlación de Pearson para las variables de hidroboya.	16

ÍNDICE DE FIGURAS

Fig 1. Ubicación del SFR, hidroboya y estación meteorológica C13.....	2
Fig 2. Gráfico climático Walter-Lieth correspondiente a la estación C13 Salve Faccha.....	5
Fig 3. A) Rosas de los vientos mensuales; y (B) rosas de viento por hora.....	6
Fig 4. Variación en el período de estudio 2019 - 2020 de los parámetros de la columna de agua.....	9
Fig 5. Distribución temporal y vertical de los diferentes parámetros de la columna de agua en el período de estudio..	10
Fig 6. Variación horaria por mapas de calor según las estaciones húmedas y relativamente secas ..	11
Fig 7. Perfiles de temperatura del SFR desde marzo de 2020 hasta abril de 2021.....	12
Fig 8. Perfiles de oxígeno disuelto del SFR desde marzo de 2020 hasta abril de 2021.....	13
Fig 9. Perfiles de clorofila-a del SFR desde marzo de 2020 hasta abril de 2021	14
Fig 10. Perfiles de pH del SFR desde marzo de 2020 hasta abril de 2021.....	14
Fig 11. Perfiles de turbidez del SFR desde marzo de 2020 hasta abril de 2021.....	15

RESUMEN

Los lagos proporcionan servicios de agua para diferentes actividades, como el suministro de agua potable a las poblaciones. Por lo cual es importante ampliar la información de los embalses para comprender su comportamiento y mejorar su gestión. El embalse Salve Faccha (SFR) en los Andes altos del Ecuador (3890 msnm) desde 1998 aporta 900 l/s al suministro de agua de Quito, lo que lo convierte en un embalse de alto interés de estudio. Busqué identificar la existencia de estratificación en el SFR mediante el análisis de la distribución temporal de los parámetros físico-químicos de los datos históricos y de la hidroboya multiparamétrica. Determine estaciones basándome en climogramas de Walter-Lieth y comportamiento de viento con rosa de los vientos. Con mapas de calor, grafique los datos de alta frecuencia previamente tratados y busque termoclinas según la densidad del agua y con los datos de muestreos mensuales, grafique isolíneas verticales. El SFR presentó leves estratificaciones térmicas estacionales (a 2.75 y 7.50m de profundidad) y químicas (entre 5 y 10m de profundidad) en la estación relativamente seca, influenciada por el viento. El oxígeno disuelto (OD) tiene una mayor variación en la columna de agua en la estación relativamente seca y sin alcanzar la anoxia. El viento influyó en la leve estratificación termoquímica horaria. La turbidez, clorofila-a, potencial de oxidación y reducción (ORP) y pH no mostraron cambios significativos o correlaciones con la temperatura y el OD. No encontré una marcada estratificación en el SFR. Sin embargo, encontré leves variaciones en la temporada relativamente seca que sugieren una tendencia a estratificación en el futuro. Estos resultados brindan información sobre las interacciones con el clima, y pueden respaldar la gestión de los reservorios y los recursos hídricos.

Palabras clave: estratificación termo-química, estacional, viento, lagos alto-andinos.

ABSTRACT

Lakes provide water services for different activities, such as supplying drinking water to populations. Therefore, it is important to expand the information on reservoirs to understand their behavior and improve their management. The Salve Faccha reservoir (SFR) in the high Andes of Ecuador (3890 masl) since 1998 contributes 900 l/s to the water supply Quito, which makes it a reservoir of high study interest. We sought to identify the existence of stratification in the SFR by analyzing the temporal distribution of the physicochemical parameters of the historical data and of the multiparametric hydrobuoy. Determine seasons based on Walter-Lieth climates and wind behavior by wind roses. Using heat maps, plot previously processed high-frequency data and search for thermoclines based on water density and with monthly sample data, plot vertical isolines. The SFR presented slight seasonal thermal stratifications (at 2.75 and 7.50m depth) and chemical (between 5 and 10m depth) in the relatively dry season, influenced by the wind. Dissolved oxygen (DO) has a greater variation in the water column in the relatively dry season and without reaching anoxia. The wind influenced the slight hourly thermochemical stratification. Turbidity, chlorophyll-a, oxidation and reduction potential (ORP) and pH did not show significant changes or correlations with temperature and DO. I did not find a marked stratification in the SFR. However, I did find slight variations in the relatively dry season that suggest a stratification trend in the future. These results provide information on interactions with climate, and can support reservoir and water resource management.

Keywords: thermo-chemical stratification, seasonal, wind, high Andean lakes.

1. INTRODUCTION

Water from rivers and lakes provide the resources for different human activities, such as agriculture, industry, and human consumption (Fernández, 2012). Reservoirs mitigate water scarcity of cities supplying water services to populations. Thus, it is necessary to understand reservoir dynamics to offer safe water (Rodríguez, 2012).

One of the major concerns for reservoirs is eutrophication since it compromises their quality of water. Lakes and reservoirs stratify due to the transfer and exchange of heat between the atmosphere and water (Cole & Weihe, 2016). Seasonal variation in temperature and precipitation influence the dynamics of these environments (Wu et al., 2020). This can cause chemical, biological and hydrological phenomena that could threaten water availability and quality (Ducharme, 2008; Ellah & Radwan, 2020). Therefore, it is important to study the physical and chemical parameters related to water quality to determine if environmental conditions affect it (Michelutti, Labaj, Grooms, & Smol, 2016).

High Andean lakes and reservoirs are usually shallow and characterized by extreme geographical locations and altitude (Albarracín et al., 2015). Over time, these environments have been affected by anthropogenic activities and their remoteness has been a limitation for studying them. In Ecuador, these ecosystems are often used as sources of water for nearby cities.

The Papallacta Oyacachi lacustrine system (POLs) is one of the primary sources of water of Quito (EPMAPS, 2020). The Salve Faccha reservoir (SFR), one of the largest in the POLs, since 1998 provides 900 l/s of water to the city, (EPMAPS, 2020) and must be constantly monitored and assessed to better know its current state and behavior. This understanding allows to establish and execute actions in relation to possible environmental phenomena that could jeopardize the provision of water of Quito. In 2016 organoleptic changes associated with cyanobacteria were detected in SFR (EPMAPS, 2020), which is why a continuous water quality monitoring system was established in 2019 by the Water Enterprise of Quito (EPMAPSQ) to know the seasonal dynamics of the different physical-chemical parameters and biological processes of the reservoir using a multiparametric hydro-buoy.

The present study aims to identify if there is stratification in the SFR by temporal distribution analysis of physical-chemical and biological parameters to predict possible effects in the water quality on the water body. The analysis of the temporal patterns of the physical parameters of the SFR contributes to expanding the information on high Andean tropical water bodies, understanding their behavior and improving their management.

2. STUDY AREA

The SFR is located in the Cayambe Coca National Park in the Napo River Basin, in the headwaters of the Amazon, at 3890 masl and 34 km East from Quito (Fig 1). The reservoir has a surface area of 137 ha and a maximum depth of 23.9 m. The most extensive land cover in the SFR's basin is scrub and grassland vegetation known as "paramo". The reservoir is fed by the Cunuyacu river and other 6 tributaries; has 12,500,000 m³, and contributes 900 L/s to the Papallacta Integrated System –PLS, part of the water supply system of Quito

(Larrea, Ríos, & Parra, 2021; Tufiño, 2011).

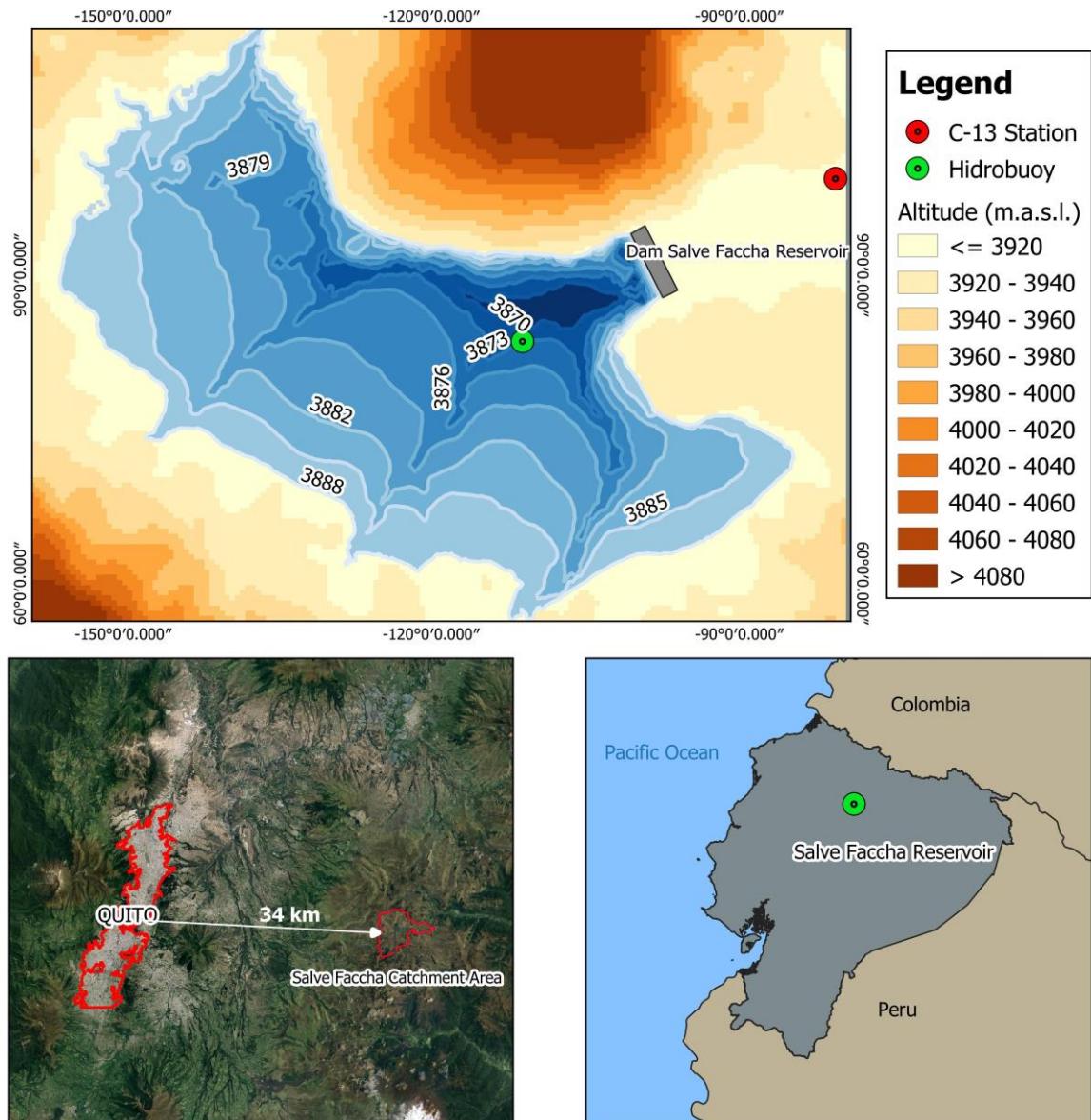


Fig 1. Bathymetry and location of the SFR, hydrobuoy, dam and C13 meteorological station.

3. MATERIALS AND METHODS

3.1. Meteorological analysis

Data for the meteorological analysis (temperature, precipitation, wind speed and wind direction) was provided by EPMAPSQ (parameter, frequency and study period are shown in table 1). Using `iki.dataclim` R package (Orlowsky, 2014), I determined the climatic conditions of the SFR basin seen in the Walter-Lieth climate graph of the “C13 Salve Faccha” meteorological station. The Walter-Lieth diagram, used in the package, plots the monthly mean values of temperature (°C) and monthly precipitation (mm) recorded at a weather station. The diagram follows the condition of the Gausson index, the axis of the right ordinate of the temperature is twice the left axis of the precipitation. This determines dry seasons if the temperature is below precipitation and wet season if it is opposite. Also, if it exceeds 100 mm, the scale increases and defines super-humid times.

Stations were defined based on sub-hourly air temperature records from 2015 to 2020 and hourly precipitation records from 2004 to 2015. In addition, I used a time series from 2019 sub-hourly wind speed and direction. The necessary exploratory data treatment finds the most complete study period, classify and group, was done before performing the monthly and hourly compass rose and the time series analysis for the study period.

3.2. Physical-chemical parameters analysis

I conducted exploratory data treatment to curate multiparametric hydro-buoy data from 2019 (temperature, dissolved oxygen, turbidity, pH, chlorophyll, and ORP). The exploratory analysis was applied with the main objective of finding the most complete study period for each parameter. After that, they were classified and grouped according to the following analyzes. I traced the variations in the parameters at different depths (0.5 m, 5 m, and 10 m) to relate them to air temperature, precipitation and wind speed time series. With the curated data I defined the time interval for each parameter used in the study.

With the `rLakeAnalyzer` R package (Read et al., 2011), I analyzed the different parameters using heat maps of the entire study period and hourly averages in the previously defined stations. Heat maps are plot with the high-frequency data completed by simple linear interpolation. It is interpolated first according to depth and then by time (Read et al., 2011). I determined the thermoclines of the water column in the days with more significant thermal variability. Thermocline depth is based on the density of the water. The density is calculated from the temperature of the water and neglecting the effects of solutes, the density is calculated according to the equation of Martin and McCutchen. Thermocline depth is defined as the one where there is the greatest change in density with respect to depth (Read et al., 2011).

Also, I calculated the Pearson correlation scores for all the bio-physical-chemical parameters at the three depths and the meteorological variables, air temperature and wind speed. Pearson correlation allows us to find the statistical linear relationship between two variables. It is used to accept the null hypothesis that there is no relationship between the analyzed variables. Values close to 0 reflect little or no linear correlation, while if the value is close to +1 it has a positive (direct) correlation; on the other hand, if it is close to -1 it has a negative (inverse) correlation (LeBlanc, 2004).

Additionally, I plot vertical isolines from non-automated monthly samplings from 2020 and 2021 of bio-physical-chemical parameters (temperature, dissolved oxygen, turbidity, pH, and chlorophyll). Isolines were classified by the meteorological stations previously defined for the sampling point at the dam and at the hydro-buoy. Additionally, water transparency from the studied period was correlated with other physical-chemical parameters.

The specifications about data used in the study are specified in Table 1.

Table 1. Characteristics of data and study period used in meteorological and physical-chemical parameters.

Parameter	Origin	Frequency	Study period
Air Temperature (°C)	C13 Salve Faccha meteorological station	sub-hourly	09/15 – 02/20
Precipitation (mm)	C13 Salve Faccha meteorological station	hourly	01/04 - 10/15
Wind speed (m/s)	C13 Salve Faccha meteorological station	sub-hourly	01/19 – 12/19
Wind direction (°)	C13 Salve Faccha meteorological station	sub-hourly	01/19 – 12/19
Temperature (°C)	hydro-buoy	sub-hourly	01/19 - 01/20
OD (mg/L)	hydro-buoy	sub-hourly	01/19 - 01/20
pH	hydro-buoy	sub-hourly	01/19 - 12/19
Turbidity (NTU)	hydro-buoy	sub-hourly	01/19 - 06/19
ORP (mV)	hydro-buoy	sub-hourly	03/19 - 12/19
Chl-a (ug/L)	hydro-buoy	sub-hourly	01/19 - 01/20
Temperature (°C)	non-automated samplings	monthly	03/20 - 04/21
OD (mg/L)	non-automated samplings	monthly	03/20 - 04/21
pH	non-automated samplings	monthly	03/20 - 04/21
Turbidity (NTU)	non-automated samplings	monthly	03/20 - 04/21
Chl-a (ug/L)	non-automated samplings	monthly	03/20 - 04/21

4. RESULTS

4.1. Meteorology

In the periods defined in table 1, I determined that the SFR had a unimodal meteorological behavior with safe frosts, temperatures below 0 °C, (June to March) and probable frost (April and May) (Fig 2). Maximum air temperature during the assessed period was 15.4 °C, minimum was -1.3 °C, and average temperature was 6.4 °C. Annual average rainfall in the area was 1228 mm, with an excess of more than 100 mm from March to July, and a highest record in June, with 145 mm. It has been recorded that June is the month with the highest rainfall, both for the period of 2006 to 2010 where March to October had rainfall between 100 to 180 mm and for the period of 2012 to 2019 where the highest precipitation occurred between April and July (Larrea et al., 2021; Tufiño, 2011).

I considered if precipitation exceeded 100 mm of monthly precipitation to define the season. Thus, from March to July corresponded to the season with the highest rainfall, while between August and February was a relatively dryer season with less than 100 mm of rainfall.

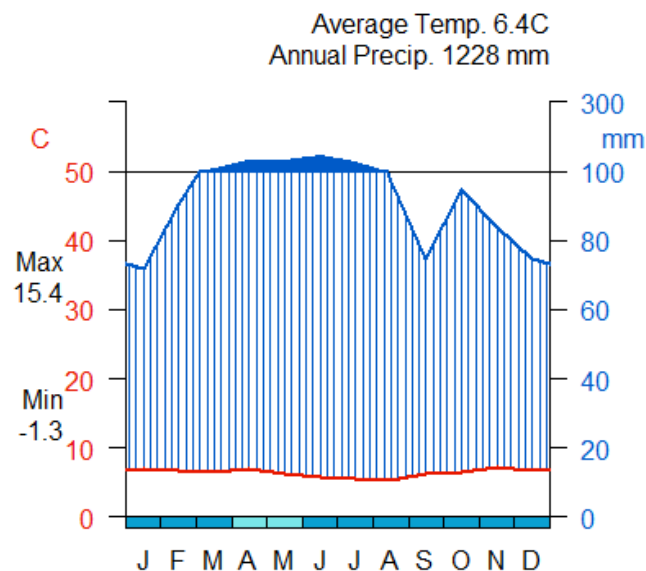
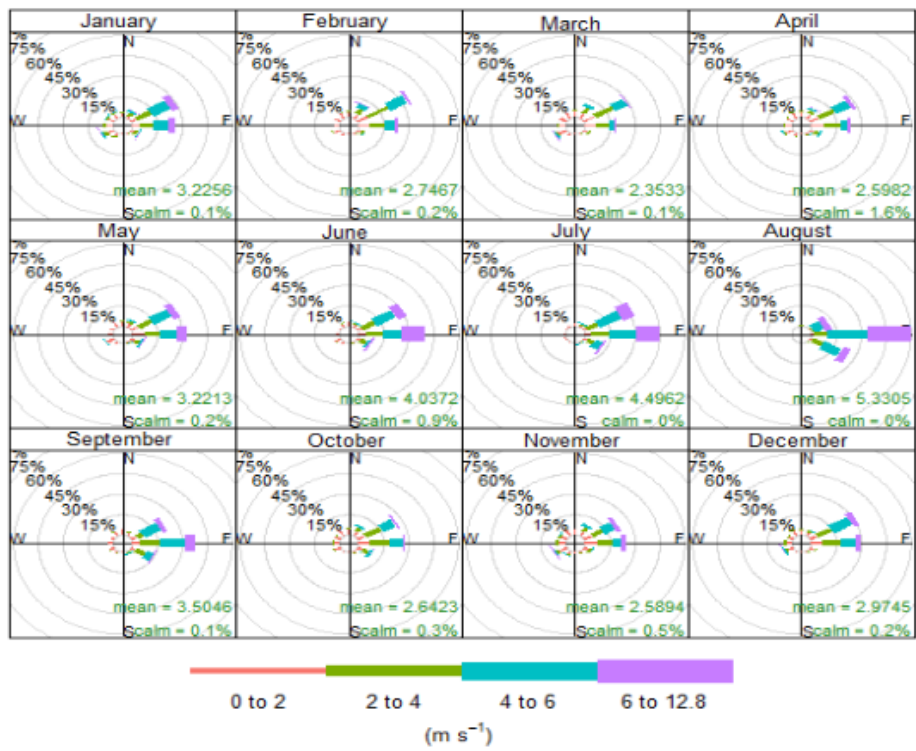


Fig 2. Walter-Lieth climate graph corresponding to the C13 Salve Faccha station. The air temperature (° C) (2015 - 2020) is marked in red and the precipitation (mm) (2004 - 2015) in blue. The x-axis in light blue shows the months in which safe frosts will be registered and in dark blue the months that are probable frost events. The dark blue area above 100 mm defines a super wet season (referred to as the wet season in this paper).

Wind speed was more intense from June to August in an Easterly direction, with August being the month with the highest average wind speed (5.33 m/s), followed by June to July with average speeds of 4.04 and 4.50 m/s, respectively. Winds come primarily from the Northeast and East throughout the year, with few wind events less than 2m/s coming from all directions (Fig 3A). At 11:00, the highest average wind speed was recorded (5.13 m/s). In general, between 8:00 and 15:00 the periods with the highest average wind were recorded mainly from the Northeast and East (Fig 3B).

A



B

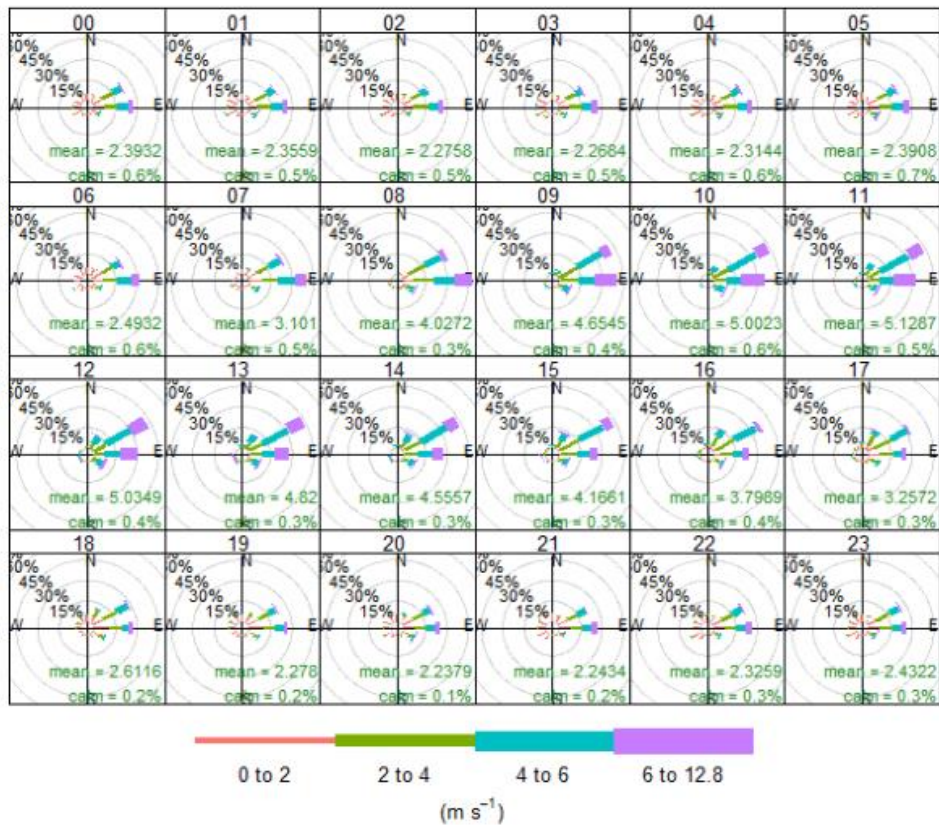


Fig 3. A) Monthly wind roses with maximum average winds between June and August; and (B) hourly wind roses with maximum winds between 8:00 and 15:00. The percentage of wind blowing in different directions, the percentage with no recorded winds, and the average wind speed for each month and hour are displayed.

4.2. High-frequency patterns of physical-chemical parameters

Water temperature decreases from April to August and from there onwards temperature increase during the study period. Water temperature in the relatively dry season in September had minor temperature variation in the water column. From June to September water temperatures were constant in the water column (wet season and the beginning of the relatively dry season) and below 9.00 °C (Fig 4A). Maximum water temperature over the study period was 12.72 °C at 0.5 m, while minimum water temperature was 6.66 °C at 10 m depth (Table 2).

The hourly water temperature in the wet season cooled down from 15:00 and began to warm up from 7:00. The hours with highest temperature ranged between 11:00 and 16:00. During these hours temperatures were above 9.60 °C up to 5m deep (Fig 6A). I found a slight tendency to thermal stratification in the months corresponding to the relatively dry season, specifically from January to March 2019 and from October 2019 to January 2020 (Fig 5A). In the relatively dry season, temperature decreased from 14:00 and increase from 8:00. Hours of maximum temperature occurred between 10:00 and 17:00, where the temperature exceeded 9.70 °C up to 5 m depth (Fig 6B).

Table 2. Summary of descriptive statistics of the data collected by the multiparametric hydrobuoy from 2019 to 2020 at three depths.

Parameter	Depth (m)	Max	Min	Mean	Median	Standard Deviation	Coefficient of variation
Temperature (°C)	0.5	12.72	6.67	9.75	9.73	1.20	0.12
	5	12.56	6.67	9.74	9.92	1.10	0.11
	10	11.35	6.66	9.33	9.38	0.93	0.10
DO (mg/L)	0.5	7.98	5.38	7.18	7.25	0.38	0.05
	5	7.72	4.60	6.95	7.07	0.53	0.08
	10	7.68	3.70	6.43	6.66	0.82	0.13
pH	0.5	7.86	5.60	6.99	7.08	0.38	0.05
	5	8.10	6.14	7.38	7.45	0.29	0.04
	10	8.05	6.78	7.36	7.36	0.27	0.04
Turbidity (NTU)	0.5	23.51	0.33	5.30	5.72	3.46	0.65
	5	26.40	0.28	5.30	5.43	3.99	0.75
	10	20.32	0.68	5.03	4.94	2.61	0.52
ORP (mV)	0.5	479.40	312.90	414.58	414.00	32.63	0.08
	5	513.40	336.40	426.11	423.50	35.11	0.08
	10	534.50	348.50	459.13	462.00	33.81	0.07
Chl-a (ug/L)	0.5	40.93	0.11	13.12	13.31	8.33	0.63
	5	40.48	2.71	17.58	17.79	6.90	0.39
	10	30.53	2.00	15.50	16.34	5.89	0.38

Dissolved oxygen (DO) had minor variation in the water column between July and October 2019, the relatively dry period (Fig 4B). It had a maximum of 7.98 mg/L (0.5 m depth) and a minimum of 3.70 mg/L (10 m depth) (Table 2). From June to September, DO had a minimal variation in the water column with values between 7.5 mg/L to 8 mg/L. The rest of the study period had more significant variation in the first months of the year until March and November (Fig 5B). Hourly DO showed an inversely proportional relationship with temperature ($r = -0.72$, $P \leq 0.01$). In the wet season DO had the lowest surface concentrations at 12:00 (Fig 6C), while in the relatively dry season it occurred at 13:00 (Fig 6D). For both seasons, the DO behavior was similar, with only a variation of 0.2 mg/L.

Turbidity did not vary between 0.5, 5 y 10m depths with means of 5.30, 5.30 y 5.03 NTU, and standard deviation of 3.46, 3.99 and 2.61 NTU respectively (Table 2); but it presented greater turbidity from February to April, with a tendency to decrease throughout the year (Fig 4C). Turbidity ranged from 0.28 NTU to 26.40 NTU (Table 2). Turbidity from January to April 2019 presented values higher than 10.00 NTU in March up to 20.00 NTU (Fig 5C). In the relatively dry season, the hourly turbidity increased below 5m between 5:00 and 15:00 in the deepest zone (Fig 6F). The water column reached the highest turbidity values higher than 3.20 NTU. In the wet season (Fig 6E), the turbidity presented greater turbidity between 8:00 and 16:00 between 3 and 7m deep, reaching 9.40 NTU.

The pH could be analyzed from February to June 2019 (Fig 4D). For the entire period, there were range from 5.60 to 8.10 (Table 2). In February and March, the pH tended to be neutral, while from April to June, it was more alkaline but tended to be neutral on the surface of the water column (Fig 5D). The hourly pH in the relatively dry season had a stable behavior at different depths at all day hours with minimal fluctuations between 9:00 and 14:00, as in the wet season (Fig 6H). However, in the wet season, a change was observed throughout the water column, with a change in behavior from 5m depth; from that depth the pH decreases with depth (Fig 6G).

The ORP changed its behavior from October, where the values fluctuate at different depths (Fig 4E). It had values range from 312.90 mV to 534.50 mV (Table 2). In the rainy season, the ORP was lower as the depth increased the ORP increases. The lowest ORP values were in October 2019, between 300.00 mV and 400.00 mV concentrated up to 5m depth. Above 500.00 mV, they were below 6m depth between May and July 2019 (Fig 5E). The ORP in the wet season was stable according to the time and increased as the depth increased (Fig 6I). In the relatively dry season, the behavior was durable with a slight variation between 9:00 and 16:00, increasing the ORP (Fig 6J).

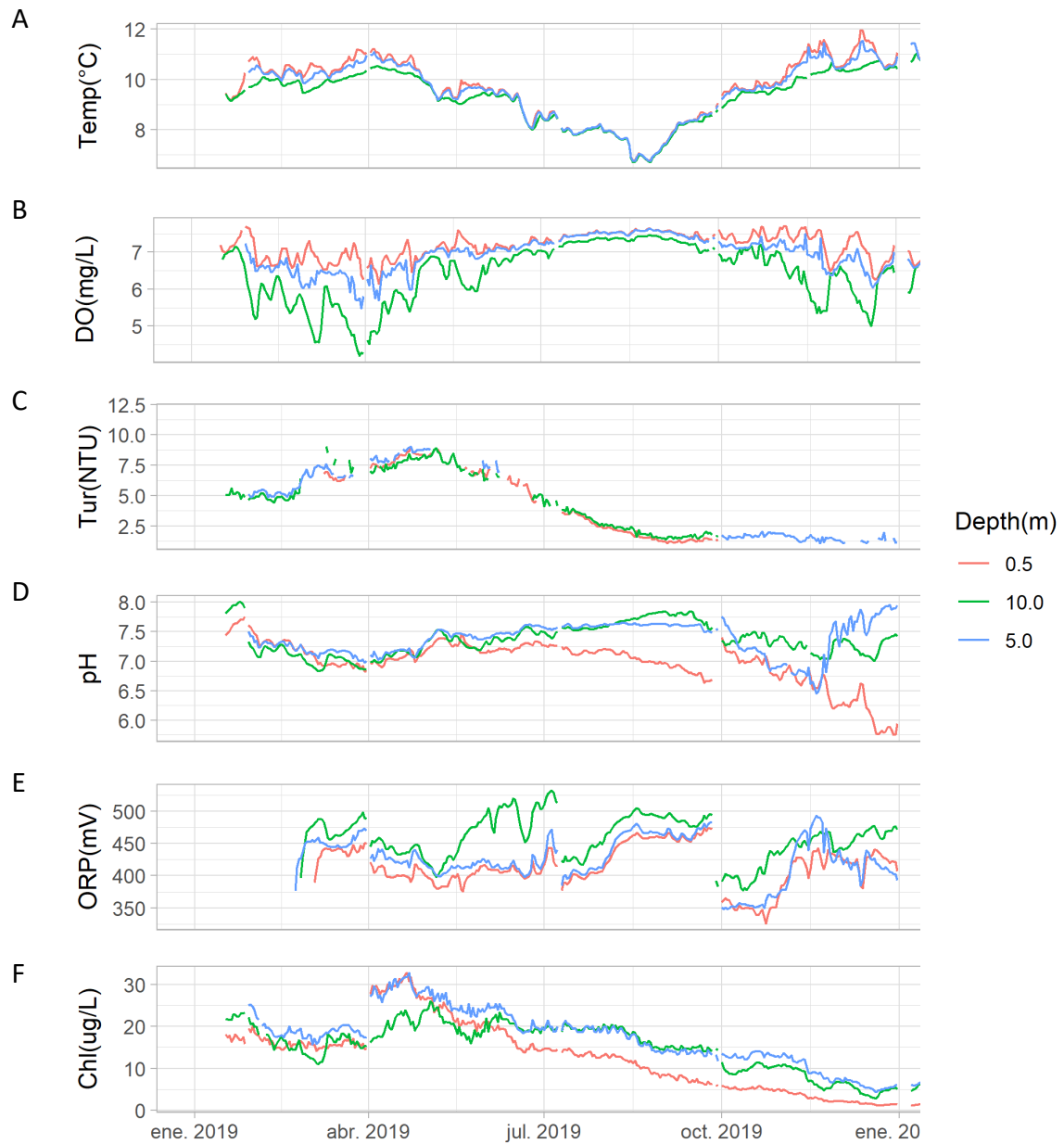


Fig 4. Variation in the study period 2019 - 2020 of the water column parameters: (A) temperature ($^{\circ}\text{C}$), (B) dissolved oxygen (mg/L), (C) turbidity (NTU), (D) pH, (E) ORP (mV), (F) chlorophyll ($\mu\text{g/L}$) at 0.5, 5, and 10m depth.

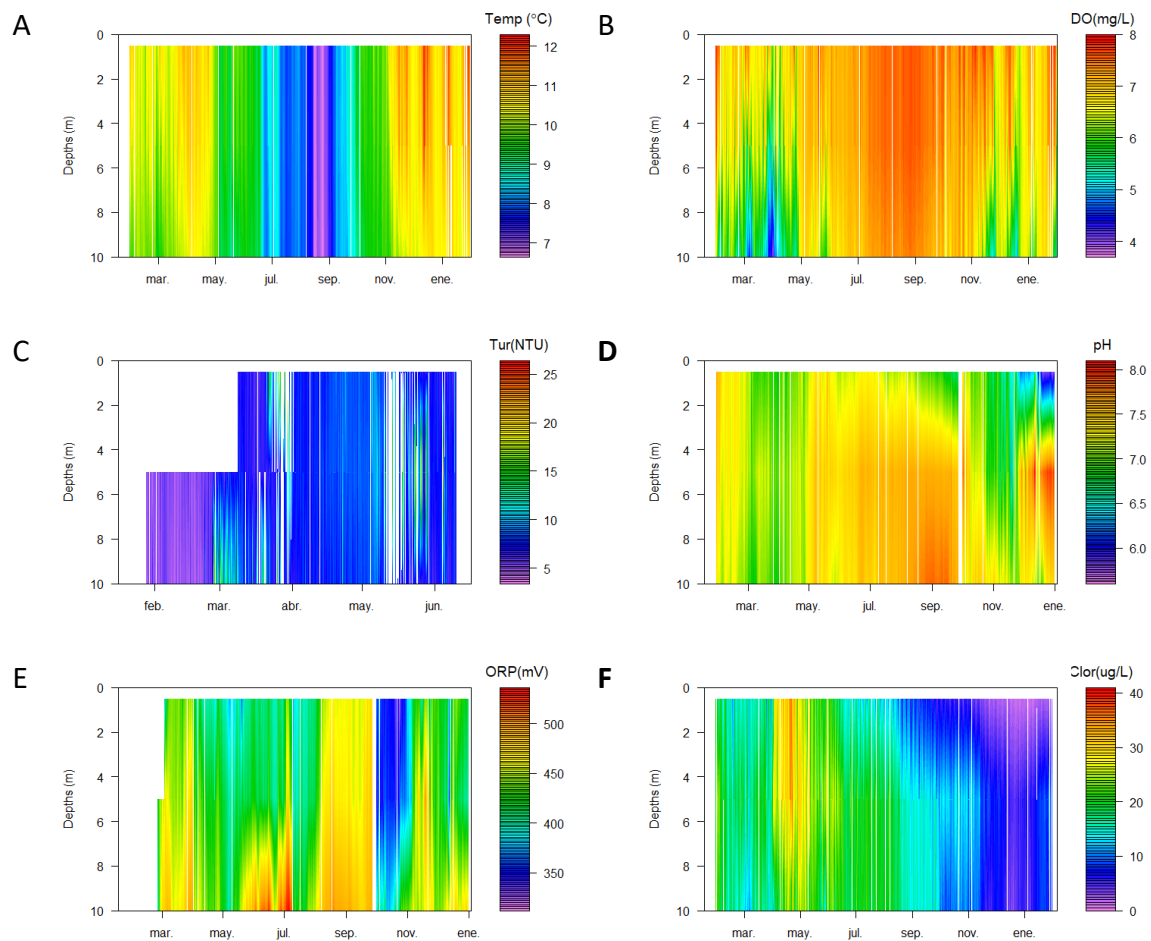


Fig 5. Temporal and vertical distribution of the different parameters of the water column in the study period A) Temperature, B) Dissolved Oxygen, C) Turbidity, D) pH, E) ORP, and F) Chlorophyll. Interpolations were done from data of 0.5, 5 and 10m depth.

Chlorophyll (Chl-a) presented a lower amount in the subsurface layer and decreased from June to December 2019. However, there was a short trend towards increasing Chl-a from January 2020 (Fig 4F). It presented values ranging from 0.11 $\mu\text{g/L}$ to 40.93 $\mu\text{g/L}$ (Table 2). In March and April 2019, Chl-a levels exceeded 25.00 $\mu\text{g/L}$, mostly exceeding 40.00 $\mu\text{g/L}$ up to 6m deep, and from that depth it descends. As of June 2019, Chl-a tended to increase as depth increases (Fig 5F). Chl-a per hour in the wet season over 5m increased as depth increased. Between 9:00 and 15:00, the lowest Chl-a values reached 17.50 $\mu\text{g/L}$. Below 5m, its behavior changed and decreased as it got deeper (Fig 6K). In the relatively dry season, between 9:00 and 16:00, the lowest levels of Chl-a were present in the water column. Below 5m, Chl-a fluctuates between 11.50 $\mu\text{g/L}$ and 13.00 $\mu\text{g/L}$ throughout the day, unlike the layer above 5m, where the variation is more remarkable, varying between 5.90 $\mu\text{g/L}$ and 13.00 $\mu\text{g/L}$ (Fig 6L).

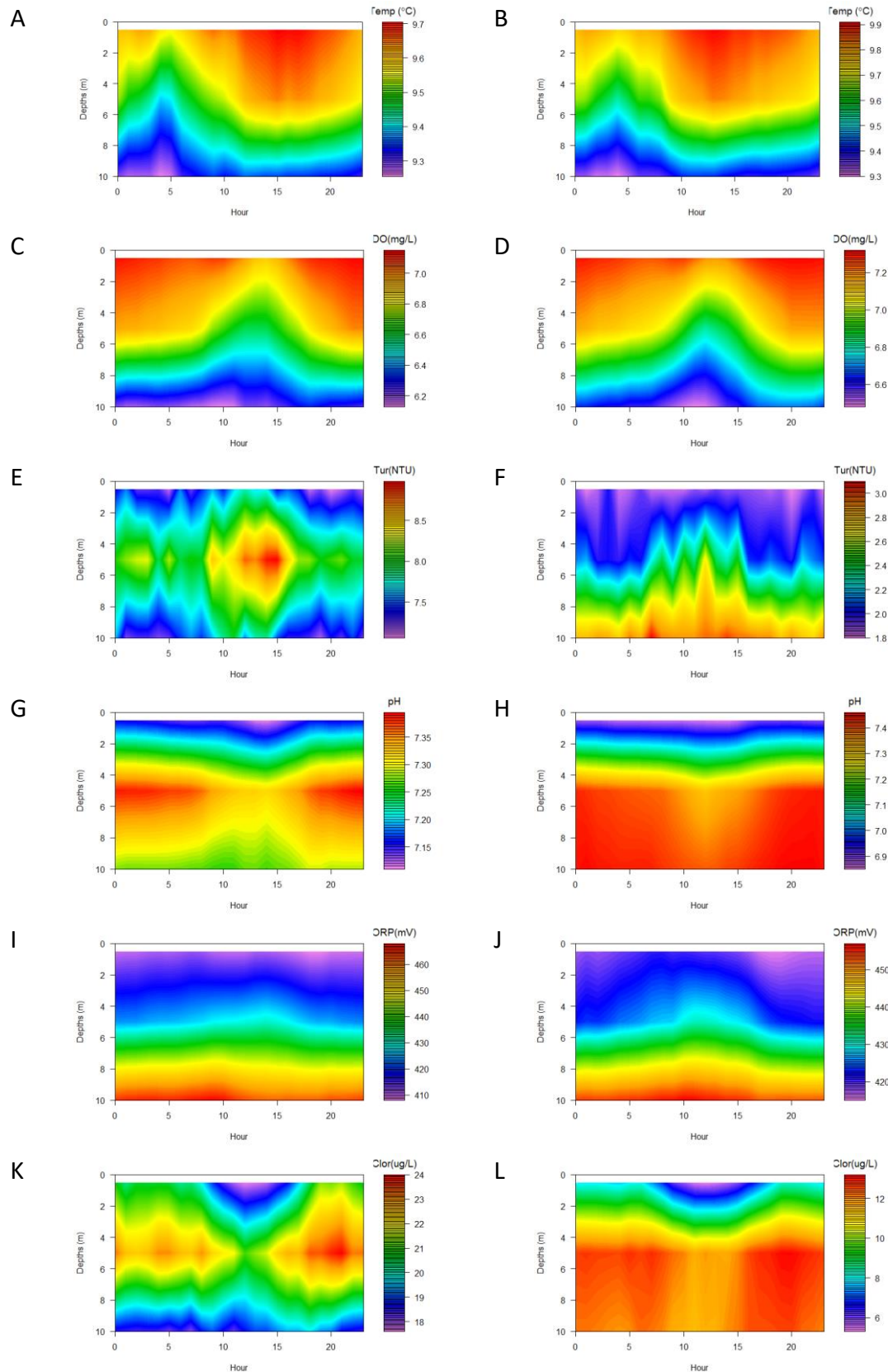


Fig 6. Hourly variation by heat maps according to the wet (left column) and relatively dry (right column) seasons. For the parameters: A) y B) Temperature, C) y D) Dissolved oxygen, E) y F) Turbidity, G) y H) pH, I) y J) ORP and K) y L) Chlorophyll.

The SFR showed thermal stratification throughout the day in the relatively dry season in the months with wind speeds lower than 4 m/s. From March, in the rainy season, the stratification began to decrease and disappeared first between 17:00 to 2:00. The thermal stratification disappeared from June to October 2019 and from February to September 2020. This stratification occurred at 2.75 and 7.50 m. The hourly temperature events were mostly concentrated from 7:00 to 16:00 and presented variations higher than 2.00 mg/L in the water column in the same months as the temperature. The hourly DO events were mostly concentrated from 5:00 to 11:00.

4.3. Monthly patterns of physical-chemical parameters

At the dam area, the reservoir is thermally stratified between September and November 2020. Surface temperature depended on the season since in the relatively dry season remained concentrated between 9.1 °C (September 2020) and 10.9 °C (October 2020), while in the wet season surface temperature was more disperse between 7.9 °C (July 2020) up to 10.9 °C (March and October 2020). Surface temperature range in the wet season represented the temperature range in the study period. Similarly, by the hydrobuoy the reservoir tended to thermally stratification in October and November 2020. The surface temperature in the relatively dry season varied between 9.3 °C (August 2020) and 11.2 °C (November 2020), while in the wet season it was between 8.0 °C (July 2020) and 10.6 °C (March 2020). The surface temperature range in the study period was between 8.0 °C and 11.2 °C (Fig 7).

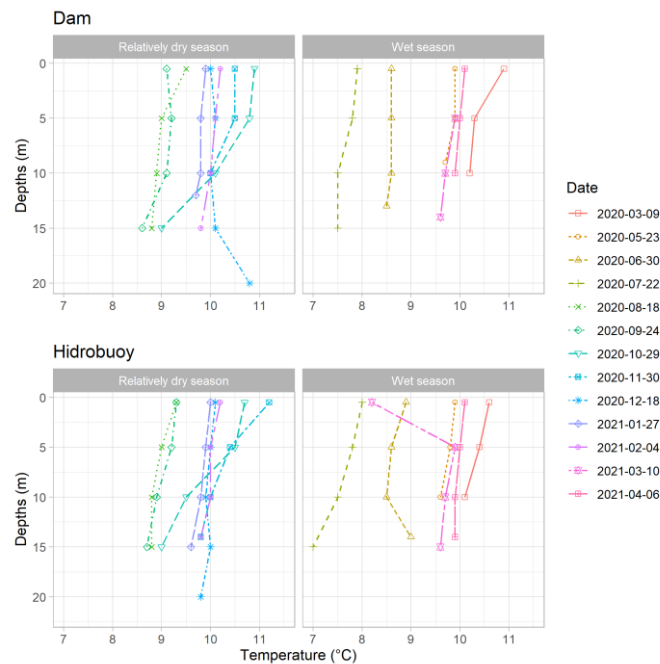


Fig 7. Temperature profiles of the SFR from March 2020 to April 2021.

A minimum DO concentration of 6.06 mg/L is on the dam's surface (December 2020), and a maximum concentration of 7.61 mg/L (August 2020). In the wet season, the surface DO is grouped between 6.95 mg/L (March 2021) and 7.29 mg/L (July 2020), while in the relatively dry season, it has a concentration of less than 6.06 mg/L (December 2020) and a maximum of 7.61 mg/L (August 2020). In December 2020, the DO concentration did not

vary until a depth of 20m. The DO in the water column is characterized by a tendency to chemical stratification at a depth of 10m (September and October 2020) both points, and in January and February 2021, the hydrobuoy at the same depth (Fig 8). The highest Chl-a concentration occurred on the surface, in hydrobuoy of 26.90 ug/L (May 2020) and 25.30 ug/L in the dam (March 2020), both in the wet season. Chl-a in the study period was between 5.50 ug/L and 25.30 ug/L in the 5.00 ug/L dam and 26.90 ug/L in the hydrobuoy (Fig 9).

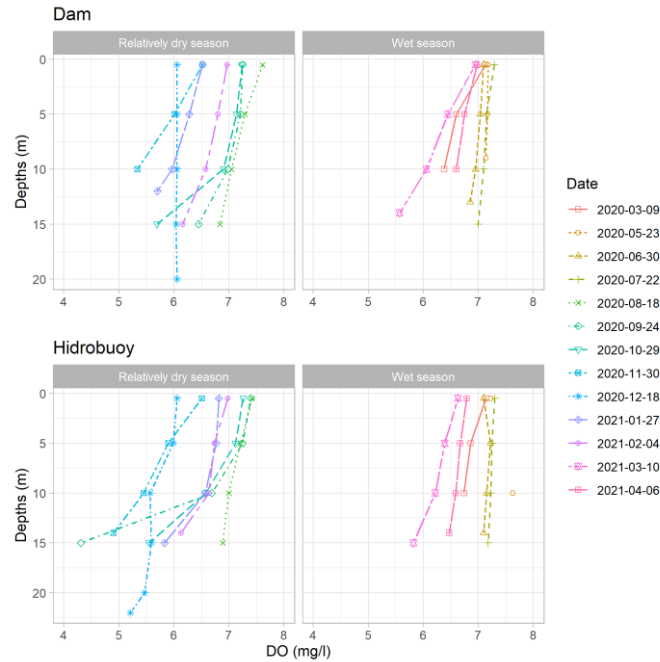


Fig 8. Dissolved Oxygen profiles of the SFR from March 2020 to April 2021.

The pH in the relatively dry season of the dam, the surface pH ranged from 7.59 (September 2020) to 8.10 (October 2020 and February 2021), and in the wet season, it varied from 7.48 (March 2020) to 8.27 (March 2021). Without presenting representative variations of the pH in the water column at any station. In the hydrobuoy in the relatively dry season, the surface pH had a minimum of 7.77 (November 2020) and higher than 8.16 (February 2021). The wet season had a minimum pH of 7.41 (May 2020) and a maximum of 8.24 (March 2021). The pH tended to be slightly higher in the surface layers (Fig 10).

I observed that turbidity was lower in the relatively dry season for both locations. In the dam, the surface turbidity varies between 9.57 NTU (December 2020) and 3.40 NTU (October 2020) in the relatively dry season, and between 8.78 NTU (March 2020) and 1.80 NTU (May 2020), in the wet season. At the point of the hydrobuoy, the surface turbidity changed from 8.61 NTU (June 2020) and 1.65 (May 2020) in the wet season, and the relatively dry season changed from 6.63 NTU (February 2021) to 3.50 NTU (October 2020). In general, turbidity remains constant and tends to increase from 10 m in the months except in June 2020 in hydrobuoy (Fig 11).

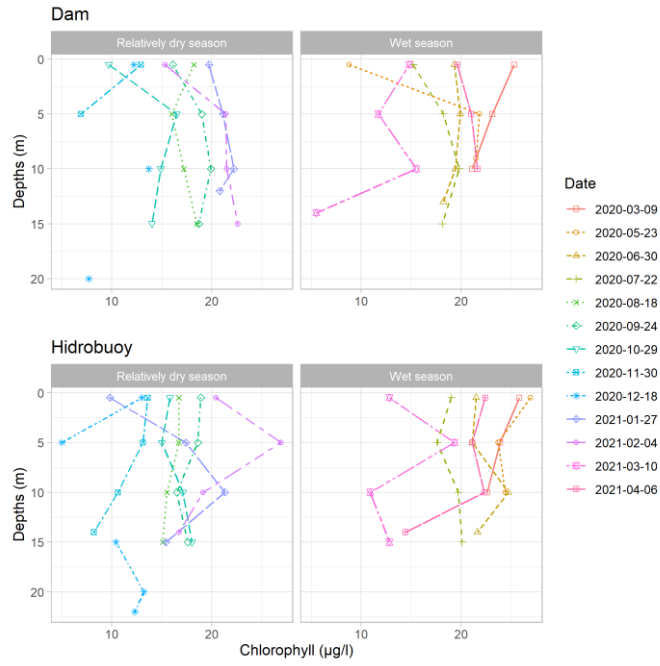


Fig 9. Chlorophyll-a profiles of the SFR from March 2020 to April 2021.

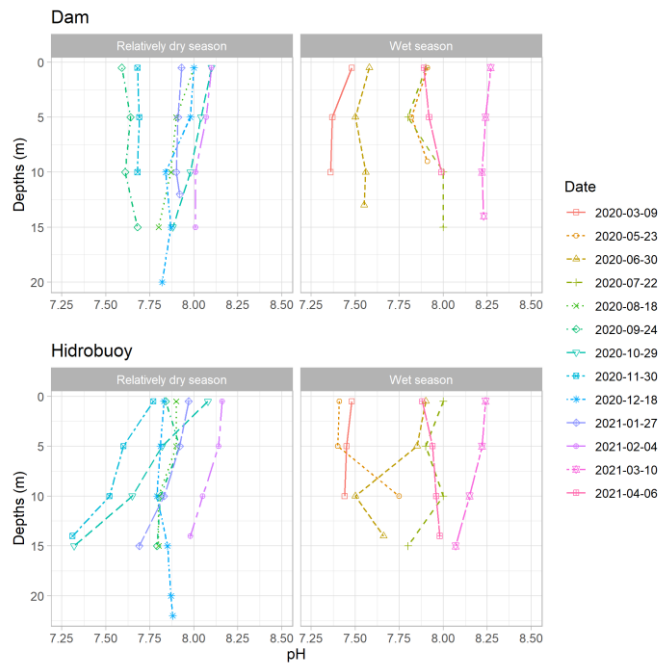


Fig 10. pH profiles of the SFR from March 2020 to April 2021.

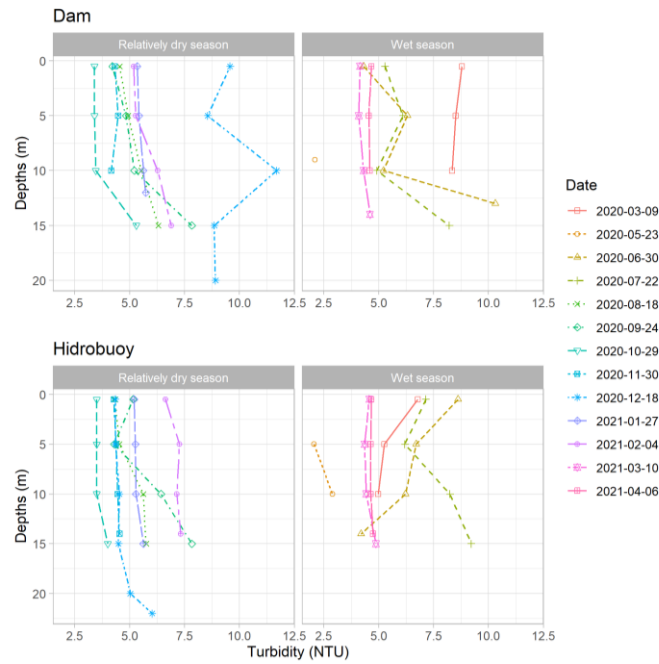


Fig 11. Turbidity profiles of the SFR from March 2020 to April 2021.

The depth of the Secchi Disk fluctuates in the relatively dry season between 0.7 and 1.5m deep. In the wet season months, May 2020 and April 2021, and in January and February, the relatively dry season reaches the highest Secchi disk depth of 1.5m. The lowest depth of 0.7m occurs in December.

4.4. Pearson correlation

For the most part, there were no significant correlations (> 0.70) between the parameters or their respective depths. Temperature had the strongest positive correlation exceeding $r = 0.95$ ($P \leq 0.01$) between its depths 0.5, 5 and 10m. DO had strong correlations except for the 0.5-10 m relationship ($r = 0.55$, $P \leq 0.01$). The pH, on the other hand, had weak positive correlations for 0.5-10 m ($r = 0.22$, $P \leq 0.01$) and 5-10 m ($r = 0.58$, $P \leq 0.01$) but weak negative correlations for 0.5-5m ($r = -0.07$, $P \leq 0.01$). Turbidity barely reaches a strong positive correlation at 0.5-10 m ($r = 0.73$, $P \leq 0.01$), but the other two positive relationships were very weak. Chl-a was a parameter with strongly positive correlations greater than $r = 0.79$ ($P \leq 0.01$). The ORP had strong positive correlations, the lowest being the 5-10m ($r = 0.68$, $P \leq 0.01$). Regarding meteorological variables, air temperature and wind had a weak positive correlation ($r = 0.27$, $P \leq 0.01$) and do not present positive or negative correlations greater than $r = 0.42$. Water temperature and wind speed were the ones with the most (negative) correlation for the three depths 0.5 ($r = -0.42$, $P \leq 0.01$), 5 ($r = -0.41$, $P \leq 0.01$) and 10m ($r = -0.36$, $P \leq 0.01$) (Table 3). Regarding the relationship between parameters, there is a strong and negative Pearson correlation in the temperature-DO and temperature-pH relationships, especially at 10m depth. The pH-DO correlates in 10-5 m and 10-10 m positively. Turbidity has strong positive correlations with temperature only at 0.5m (on average $r = 0.74$, $P \leq 0.01$) and slightly weak at 10m (on average $r = 0.66$, $P \leq 0.01$). There is a strongly negative correlation ($r = -0.75$, $P \leq 0.01$) present between turbidity (0.5m) and pH (10m). Chl-a has strong positive relationships with pH at 0.5m; however, all other depths become weak and negative. Chl-a with turbidity has a strongly positive correlation at 0.5-5m respectively (Table 3).

Table 3. Pearson's correlation for hydro-buoy variables (water temperature, dissolved oxygen, chlorophyll-a, pH, turbidity, and ORP) at 0.5, 5, and 10m; and meteorological variables (air temperature and wind speed).

Parameter	Depth	Temperature (°C)			DO (mg/L)			pH			Turbidity (NTU)			ORP (mV)			Chl-a (ug/L)			Air Temperature (°C)	Wind Velocity (m/s)	
		0.5	5.0	10.0	0.5	5.0	10.0	0.5	5.0	10.0	0.5	5.0	10.0	0.5	5.0	10.0	0.5	5.0	10.0			
Temperature (°C)	0.5	1.00																				
	5.0	0.99	1.00																			
	10.0	0.95	0.97	1.00																		
DO (mg/L)	0.5	-0.41	-0.48	-0.54	1.00																	
	5.0	-0.63	-0.60	-0.66	0.77	1.00																
	10.0	-0.72	-0.70	-0.68	0.55	0.79	1.00															
pH	0.5	-0.33	-0.36	-0.36	0.25	0.26	0.20	1.00														
	5.0	-0.50	-0.48	-0.46	0.17	0.42	0.50	-0.07	1.00													
	10.0	-0.80	-0.85	-0.74	0.53	0.78	0.90	0.22	0.58	1.00												
Turbidity (NTU)	0.5	0.75	0.74	0.74	-0.60	-0.66	-0.68	0.29	-0.66	-0.75	1.00											
	5.0	-0.23	-0.23	-0.23	-0.27	-0.22	-0.25	0.49	0.01	-0.19	0.09	1.00										
	10.0	0.66	0.66	0.65	-0.54	-0.62	-0.61	0.12	-0.64	-0.67	0.73	0.18	1.00									
ORP (mV)	0.5	-0.25	-0.25	-0.26	-0.10	-0.02	-0.04	-0.30	0.20	0.19	-0.51	0.13	-0.48	1.00								
	5.0	-0.14	-0.17	-0.20	-0.04	-0.12	-0.17	-0.14	-0.10	0.03	-0.39	0.23	-0.27	0.89	1.00							
	10.0	-0.22	-0.24	-0.26	0.01	0.02	-0.06	-0.06	0.19	0.10	-0.23	0.20	-0.17	0.72	0.68	1.00						
Chl-a (ug/L)	0.5	-0.08	-0.06	-0.05	-0.24	-0.18	-0.21	0.61	-0.11	-0.17	0.65	0.73	0.52	-0.11	0.02	0.00	1.00					
	5.0	-0.20	-0.19	-0.18	-0.10	-0.02	-0.08	0.70	-0.10	-0.10	0.58	0.69	0.43	-0.16	-0.03	-0.02	0.92	1.00				
	10.0	-0.46	-0.46	-0.42	0.03	0.15	0.22	0.75	0.10	0.27	0.32	0.68	0.11	0.01	0.07	0.11	0.79	0.85	1.00			
Air Temperature (°C)		0.30	0.27	0.31	-0.21	-0.40	-0.26	-0.11	-0.24	-0.28	0.32	0.04	0.28	0.00	0.08	-0.03	-0.09	-0.08	-0.11		1.00	
Wind Speed (m/s)		-0.42	-0.41	-0.36	-0.04	0.10	0.32	0.07	0.28	0.33	-0.23	0.04	-0.23	0.11	0.03	0.12	-0.11	-0.06	0.13		0.27	1.00

5. DISCUSSION

5.1. High-frequency patterns of physical-chemical parameters

With high-frequency data I identified stratification during the relatively dry season, when there is lower wind speed and larger daily temperature variation. Ambient temperature influences water temperature directly and makes the SFR mix completely between June and September, but also causes a slight thermal stratification the rest of the year. The SFR, close to 4000 msl and presenting low ambient temperatures throughout the year requires less wind power to mix the water column (Tufiño, 2011). The wind that is present throughout the year produces this behavior. Its influence is more noticeable in August (the beginning of the relatively dry season). The complete mixture occurred when the water and air temperatures recorded were the lowest.

There are depth-dependent thermal stratifications (Roldán & Ramírez, 2008) in the months defined as the relatively dry season. To a lesser extent and occasionally, there are thermal stratifications in March, April, and May. According to the wind record, the months in which there are no thermal stratifications (June, July, and August) record average winds greater than 4m/s generating mixture in the water column and avoiding the formation of thermal stratifications (Darbyshire & Edwards, 1972; Klaić, Babić, & Orlić, 2020). Thermal stratifications are mostly found at 7.5 m depth, presenting variations of up to 2.36 °C from the surface to 10 m depth. This behavior suggests that the SFR has a slight tendency to seasonal thermal stratification influenced by wind events.

Although the daily variations do not exceed 0.4 °C difference, the most homogeneous layer, formed up to 5m, occurs between 10:00 to 17:00, which corresponds to the hours of highest ambient temperature in the day and especially coincides with the hours of greatest average winds between 3.25 m/s and 5.13 m/s. When winds diminish after 16:00, the most homogeneous layer of temperature in the water is lost.

With the characteristics mentioned above of elevation and location of the SFR, this is polymictic (Wetzel, 2001) with a period of slight stratification and cooling periods where complete mixing is up to 10 m depth influenced by the wind, this being an essential factor for the circulation of tropical lakes (Lewis, 1996; Nilssen, 1984). The hourly behavior is the same for the relatively dry and wet seasons without a marked stratification. It is essential to emphasize the more homogeneous layer of the water column (5m) and the direct relationship of the wind with the mixture. The temperature in the water column is relatively constant (without sudden changes) in the wet season and with a slight tendency to stratify below 5 or 10 m in the relatively dry season. This behavior agrees with those recorded by the hydro-buoy, which suggests that the strong winds present in the wet season allow mixing in the water column (Lewis, 1996; Nilssen, 1984).

The turbidity follows the same pattern of increase or decrease temperatures. As for the hourly turbidity increases with depth, but in the rainy season there is a change in behavior from a depth of 5 m probably due to a more significant amount of precipitation, leading to water with lower temperatures and sediments entering the reservoir (Elçi, 2008). The pH has a negative relationship to the water temperature in the study period, which may be

due to factors such as photosynthetic, oxidative, among others (Arocena et al., 1999; Cole & Weihe, 2016). In the relatively dry season, the pH presents a distribution with minimal changes throughout the day, increasing pH as it deepens. There is also a slight alteration between 8:00 and 16:00, since, below 5m of depth, it does not increase as fast as in the rest of the day. From 5m to 10m, the pH values remain more constant than in the upper layer in the relatively dry season, which changes in the wet season. There is no significant due to pH has a decrease of only 0.10. In the period of the greater stability of the pH (February to July 2019) and the hourly distribution, there are no variations more significant than one unit between the surface and 10m of depth. The sampling data show changes in the pH of October and November in the hydrobuoy.

DO repeats the behavior of the water temperature in terms of the months and hours in which it tends of stratification and repeats the influence of the wind. In the water column, both parameters decrease as it gets deeper without reaching anoxia, which is a characteristic of oligotrophic lakes (Garbacz, Cieściński, Ciechalski, Dąbkowski, & Cichowska, 2018). However, the seasonal events found lead to the reservoir being mesotrophic, as already mentioned by Tufiño (2011). DO concentration and water temperature show inversely proportional behavior throughout the study period. The period of most outstanding mixing of DO was recorded between July to September (mostly belonging to the relatively dry season) as in the water temperature parameter, and the rest of the months with slight stratification tendencies. The predominance of the mixture in the water column, in this case, responds to the ambient temperature and the wind being more noticeable up to 5m since the variation is less than the variation between 5 to 10 m of depth. Exist uniformity and a higher concentration of DO in the time of higher rainfall, lower ambient temperature, and high average winds. In addition, there is a higher concentration of DO in the upper layers. There is a tendency to stratification, which coincides with lower wind speeds in the relatively dry season. The maximum hourly concentration of DO varies 0.20 mg/L between seasons and is lower between 8:00 and 16:00, coinciding with higher water temperatures and stronger winds. For the study period and the depths analyzed, the reservoir does not present any case of anoxia since it does not settle in a highly intervened area without being exposed to pollutants such as sewage or nutrients from crop fields (Roldán & Ramírez, 2008). DO in general remains mixed with slight tendencies to stratify in the relatively dry season, and concentrations ranged between 6.00 mg/L to 8.00 mg/L considered typical values in uncontaminated waters. In addition, the periodic mixing in the water column and the influence of the wind is considered a good sign for the excellent condition of the reservoir (Tufiño, 2011; Wetzel, 2001).

The ORP has an oxidizing behavior in the water column and increases as it deepens throughout the study period at pH between 6.00 and 8.00, which suggests stable photosynthetic activity at depth along with the absence of anoxia (Koretsky, MacLeod, Sibert, & Snyder, 2011; Rangel, De Anda, González, & Erickson, 2009). However, the hydrobuoy data show discontinuity in July and October 2019. From July to October 2019, the ORP values are within the behavior of the previous months, but at the beginning of October, the lowest values recorded are lower at 350.00 mV.

In the relatively dry season, turbidity values are lower than in the wet season and tend to

have a linear behavior throughout the day with a slight increase between 8:00 and 16:00, when wind is most potent. Despite this observation, wind does not show direct influence by turbidity. On the other hand, in the analysis period, the Chl-a levels are around 40.00 ug/L. However, because there is a mixture in the reservoir, there is no phytoplankton growth in most of the period (Tufiño, 2011). Winds and temperature are not related to Chl-a, but it is related to turbidity (Atique & An, 2019) and tends to decrease in the same months.

5.2. Monthly patterns of physical-chemical parameters

Water temperature at the dam and at the hydro-buoy showed similar behaviors in the water column. The temperature variations between surface and bottom (15m) in the wet season did not exceed the average of 0.5 °C, except for the surface temperature of March 10, 2020, in the hydro-buoy. The recorded weather conditions (weak winds) in that month suggest less mixing (Mi, Frassl, Boehrer, & Rinke, 2018; Nilssen, 1984). However, this outlier could be due to external factors. In the same way, in the relatively dry season variations between points did not exceed 0.5 °C. In general, there is greater mixture in the wet season, although in 22 July 2020 I noticed a marked tendency to decrease, as most isolines in the relatively dry season that tend to have a slight stratification. This behavior could be because July was previously established as the limit between seasons, being a month of transition. This observation is repeated in January and February 2021, since their isolines are technically straightforward and occur in the relatively dry season. This is not a similar to the previous case since as it is not within the limit established by the seasons, but rather could be due to the weather conditions of the day and the time the data was recorded. However, there are no records in this regard.

In the wet season, DO shows the same behavior in the dam and the hydrobuoy with differences of less than 0.50 mg/L between sampling depths, especially on the surface where the data vary more than in the wet season. In the relatively dry season on the surface, it behaves the same as in the other season. Still, after 10m, its behavior changes, and there is a more significant decrease in oxygen in the hydro-buoy. The tendency to decrease in the relatively dry season (except December in the dam) is more marked than in the wet season. This more significant trend and behavior in the relatively dry season suggests an occasional seasonal stratification (Toller et al., 2020).

Chl-a does not present a defined behavior but presents higher concentrations in the wet season for dam and hydrobuoy. It is within the range of concentrations found in the hydrobuoy data. However, in the in situ data, it does not exceed 27.00 ug/L, while in the hydrobuoy, higher events are found in April to June 2019 in the wet season, which may be due to a load of nutrients in the bottom due to precipitation (Jiang et al., 2019; Rangel et al., 2009). The reservoir is mesotrophic since it presents average levels of Chl-a from 2.50 to 8.00 ug/L with maximums ranging from 25.00 ug/L (Rangel et al., 2009), taking into consideration only the in-situ data. For both points, the samplings of August and September 2019 and March 2021 have the slightest variation of Chl-a in the water column, and these same months present constant temperatures in the water column; that is, it is mixed, which can reduce the growth of phytoplankton in the water column (Marques et al., 2005; Serra et al., 2007; Wu et al., 2014).

The pH is between 8.27 and 7.31, without significant variations between hydrobuoy and dam. In the dam, the pH is more uniform with maximum variations of 0.22 in the water column. On the other hand, the hydrobuoy presents variation up to 0.76. Both extremes are from October 2020 in the relatively dry season, but it is recommended for drinking and natural waters (Roldán & Ramírez, 2008; Teame & Zebib, 2016). The pH is stable in the water column in the dam; in the hydrobuoy, it presents isolated events that exceed a change of 0.25 in the water column (May 2020, October 2020, and November 2020). The pH profiles change their behavior to splitting at 5 or 10m. However, the variation does not exceed 1.00 between surfaces, characteristic of polymictic high mountain lakes (Roldán & Ramírez, 2008; Song et al., 2021).

Turbidity in the relatively dry season increases from a depth of 10 m in the study period except for February 2021 in the dam and September 2020 in the hydrobuoy, which begin to increase from 5m. In this season in the dam, there is a considerable decrease from 5m (December 2020), but at 15m, it returns to values close to the one marked at 5m. There are more variable turbidity behaviors in the wet season than in the other season, especially in June 2020 in the hydrobuoy, since the turbidity decreases as the temperature increases. Also, in the dam in June and July 2020, and the hydrobuoy in July 2020, turbidity increases significantly from 10m, which is because the sampling could be after a precipitation event, which would imply sediment drag that persists at that depth (Elçi, 2008; Umeda & Kobor, 2019).

In the study period, the average Secchi disc transparency is 1.16m. In the wet season, it was 1.20m, and in the relatively dry season, it was 1.13m. The variation of the transparency between seasons is only 0.07m, considering several factors such as the observer's view, the shadow of the boat, weather conditions, or the brightness of the water surface, this variation is not representative (Roldán & Ramírez, 2008; Smith, 2001).

6. CONCLUSION

The SFR presents a unimodal precipitation regime and for ease of study a wet season and a relatively dry one established.

It presents slight seasonal thermal (at 2.75 and 7.50 m depth) and chemical stratifications (between 5 and 10 m depth) in the relatively dry season influenced by winds less than 4 m/s. Hourly thermal and chemical stratification events were mostly concentrated from 7:00 to 16:00.

Turbidity, chlorophyll-a, ORP, and pH do not show significant changes or correlations with the temperature and dissolved oxygen of the water column.

In general, a marked stratification is not observed in the SFR. However, slight variations are found in the relatively dry season that suggest a stratification trend in the future.

7. ACKNOWLEDGEMENTS

This research was possible thanks to a grant and data from ECAP - Water and Paramo

8. REFERENCES

- Albarracín, V. H., Kurth, D., Ordoñez, O. F., Belfiore, C., Luccini, E., Salum, G. M., ... Farías, M. E. (2015). High-Up: A Remote Reservoir of Microbial Extremophiles in Central Andean Wetlands. *Frontiers in Microbiology*, 6. doi: 10.3389/fmicb.2015.01404
- Arocena, R., Aubriot, L., Bonilla, S., Chalar, G., Conde, D., Daners, G., ... Scasso, F. (1999). *Métodos en Ecología de Aguas Continentales*.
- Atique, U., & An, K. G. (2019). Reservoir water quality assessment based on chemical parameters and the chlorophyll dynamics in relation to nutrient regime. *Polish Journal of Environmental Studies*, 28(3), 1043–1061. doi: 10.15244/pjoes/85675
- Cole, G. A., & Weihe, P. E. (2016). *Textbook of limnology* (Fifth Edition). Waveland Press.
- Darbyshire, J., & Edwards, A. (1972). Seasonal formation and movement of the thermocline in lakes. *Pure and Applied Geophysics PAGEOPH*, 93(1), 141–150. doi: 10.1007/BF00875230
- Ducharne, A. (2008). Importance of stream temperature to climate change impact on water quality. *Hydrology and Earth System Sciences*, 12(3), 797–810. doi: 10.5194/hess-12-797-2008
- Elçi, Ş. (2008). Effects of thermal stratification and mixing on reservoir water quality. *Limnology*, 9(2), 135–142. doi: 10.1007/s10201-008-0240-x
- Ellah, A., & Radwan, G. (2020). Physical properties of inland lakes and their interaction with global warming: A case study of Lake Nasser, Egypt. *The Egyptian Journal of Aquatic Research*, 46(2), 103–115. doi: 10.1016/j.ejar.2020.05.004
- EPMAPS. (2020). *BASES DE POSTULACIÓN PROGRAMA DE BECAS – CONVOCATORIA 2020 ESTACIÓN CIENTÍFICA AGUA Y PÁRAMO* (p. 19). p. 19. Quito.
- Fernández, A. (2012). El agua: un recurso esencial. *Química Viva*, 11(3), 147–170.
- Garbacz, J. K., Cieściński, J., Ciecchalski, J., Dąbkowski, R., & Cichowska, J. (2018). Thermal and Oxygen Conditions of Lake Charzykowskie in the Years 2014-2016. *Polish Hyperbaric Research*, 62(1), 85–96. doi: 10.2478/phr-2018-0007
- Jiang, W. W., Yu, J. S., Li, Z. J., Nakamura, T., Yu, F. Q., & Zhang, J. Y. (2019). Spatial variation of within-day and between-day chlorophyll a dynamics during summer in guanting reservoir, Beijing, China. *Applied Ecology and Environmental Research*, 17(3), 5765–5780. doi: 10.15666/aeer/1703_57655780
- Klaić, Z., Babić, K., & Orlić, M. (2020). Evolution and dynamics of the vertical temperature profile in an oligotrophic lake. *Hydrology and Earth System Sciences*, 24(7), 3399–3416. doi: 10.5194/hess-24-3399-2020
- Koretsky, C. M., MacLeod, A., Sibert, R. J., & Snyder, C. (2011). Redox Stratification and Salinization of Three Kettle Lakes in Southwest Michigan, USA. *Water, Air, & Soil Pollution* 2011 223:3, 223(3), 1415–1427. doi: 10.1007/S11270-011-0954-Y
- Larrea, P. P., Ríos, X. Z., & Parra, L. C. (2021). Application of neural network models and anfis for water level forecasting of the salve faccha dam in the andean zone in Northern Ecuador. *Water (Switzerland)*, 13(15), 2011. doi: 10.3390/w13152011
- LeBlanc, D. (2004). *Statistics: Concepts and Applicatios for Science*.
- Lewis, W. M. (1996). Tropical lakes: how latitude makes a difference. *Perspectives in Tropical Limnology*, 43–64.
- Marques, M., Bicudo, C., & Ferragut, C. (2005). Short term spatial and temporal variation of phytoplankton in a shallow tropical oligotrophic reservoir, southeast Brazil. In *Aquatic Biodiversity II* (pp. 235–247). doi: 10.1007/1-4020-4111-x_23
- Mi, C., Frassl, M. A., Boehrer, B., & Rinke, K. (2018). Episodic wind events induce persistent shifts in the thermal stratification of a reservoir (Rappbode Reservoir, Germany). *International*

- Review of Hydrobiology*, 103(3–4), 71–82. doi: 10.1002/iroh.201701916
- Michelutti, N., Labaj, A. L., Grooms, C., & Smol, J. P. (2016). Equatorial mountain lakes show extended periods of thermal stratification with recent climate change. *Journal of Limnology*, 75(2), 403–408. doi: 10.4081/jlimnol.2015.1444
- Nilssen, J. P. (1984). Tropical lakes - functional ecology and future development: The need for a process-orientated approach. *Hydrobiologia*, 113(1), 231–242. doi: 10.1007/BF00026611
- Orlowsky, B. (2014). *iki.dataclim: Consistency, Homogeneity and Summary Statistics of Climatological Data. R package version 1.0.*
- Rangel, J. G., De Anda, J., González, F. A., & Erickson, D. E. (2009). Water quality assessment of Aguamilpa Reservoir, Nayarit, Mexico. *WIT Transactions on Ecology and the Environment*, 125, 169–183. doi: 10.2495/WRM090161
- Read, J. S., Hamilton, D. P., Jones, I. D., Muraoka, K., Winslow, L. A., Kroiss, R., ... Gaiser, E. (2011). Derivation of lake mixing and stratification indices from high-resolution lake buoy data. *Environmental Modelling and Software*, 26(11), 1325–1336. doi: 10.1016/j.envsoft.2011.05.006
- Rodríguez, F. (2012). *DISEÑO DE LA OBRA DE CIERRE Y LAS OBRAS COMPLEMENTARIAS EN EL EMBALSE PAMPAS DE SALASACA.*
- Roldán, G., & Ramírez, J. J. (2008). *FUNDAMENTOS DE LIMNOLOGIA NEOTROPICAL* (Vol.15; Universidad de Antioquia, Ed.).
- Serra, T., Vidal, J., Casamitjana, X., Soler, M., & Colomer, J. (2007). The role of surface vertical mixing in phytoplankton distribution in a stratified reservoir. *Limnology and Oceanography*, 52(2), 620–634. doi: 10.4319/lo.2007.52.2.0620
- Smith, D. (2001). A Protocol for Standardizing Secchi Disk Measurements, Including Use of a Viewer Box. *Lake and Reservoir Management*, 17(2), 90–96. doi: 10.1080/07438140109353977
- Song, Z., Song, G., Tang, W., Zhao, Y., Yan, D., & Zhang, W. (2021). Spatial and temporal distribution of Mo in the overlying water of a reservoir downstream from mining area. *Journal of Environmental Sciences*, 102, 256–262. doi: 10.1016/j.jes.2020.09.033
- Teame, T., & Zebib, H. (2016). Seasonal Variation in Physico-Chemical Parameters of Tekeze Reservoir, Northern Ethiopia. *Animal Research International*, 13(2), 2413–2420. doi: 10.4314/ari.v13i2.
- Toller, S., Giambastiani, B. M. S., Greggio, N., Antonellini, M., Vasumini, I., & Dinelli, E. (2020). Assessment of Seasonal Changes in Water Chemistry of the Ridracoli Water Reservoir (Italy): Implications for Water Management. *Water (Switzerland)*, 12(2), 581. doi: 10.3390/w12020581
- Tufiño, P. (2011). *Planes de manejo de los embalses Salve Faccha, Sucus y Mogotes.*
- Umeda, M., & Kobor, B. (2019). VERTICAL STRUCTURE OF VELOCITY DISTRIBUTIONS MEASURED IN A THERMALLY STRATIFIED RESERVOIR. *38th IAHR World Congress - "Water: Connecting the World,"* 38, 5131–5136. doi: 10.3850/38wc092019-1559
- Wetzel, R. G. (2001). Limnology: Lake and River Ecosystems. In *Journal of Phycology* (Vol. 37).
- Wu, Y., Fang, H., Huang, L., & Ouyang, W. (2020). Changing runoff due to temperature and precipitation variations in the dammed Jinsha River. *Journal of Hydrology*, 582, 124500. doi: 10.1016/j.jhydrol.2019.124500
- Wu, Z., He, H., Cai, Y., Zhang, L., & Chen, Y. (2014). Spatial distribution of chlorophyll a and its relationship with the environment during summer in Lake Poyang: A Yangtze-connected lake. *Hydrobiologia*, 732(1), 61–70. doi: 10.1007/s10750-014-1844-2